Axin2^{+} PDL Cells Directly Contribute to New Alveolar Bone Formation in Response to Orthodontic Tension Force

K. Wang, C. Xu, X. Xie, Y. Jing, P. Chen, S. Yadav, Z. Wang, R.W. Taylor, J. Wang, and J.Q. Feng

Appendix

Supplementary Methods

Tissue Preparation, Histology, and Immunostaining

Both left and right maxillae were collected. Samples from *Axin2*$^{lacZ/+}$ mice were fixed in 0.2% glutaraldehyde at 4°C overnight and decalcified in 10% ethylenediaminetetraacetic acid (EDTA) with 2 mM $MgCl_2$ at 4°C for 2 weeks, followed by X-gal staining (Men et al. 2020).

For all the other transgenic mice, maxillae were fixed in 4% paraformaldehyde in phosphate-buffered saline (pH=7.4) overnight. Non-decalcified maxillae were dehydrated in ascending graded ethanol (75%, 95%, and 100% for twice, 2-4 days each) followed by xylene, embedded in methyl-methacrylate (MMA, Buehler, Lake Bluff, IL), cut into 10 μm-thick sections (Leica Polycut S microtome) to examine the fluorochrome labeling as previously describes(Zhang et al. 2015). Decalcified (10% EDTA) samples for histology were embedded in paraffin, sectioned, and stained with alkaline phosphatase (ALP), tartrate-resistant acid phosphatase (TRAP), or pentachrome staining as previously reported (Leucht et al. 2007). Decalcified samples for cell lineage tracing were dehydrated with 30% sucrose, embedded in OCT compound (Sakura Tissue-Tek), and cut to 10-μm-thick sections with a Leica cryostat. Immunostaining was proceeded with the following antibodies: anti–β-catenin mouse monoclonal antibody (PY489, DSHB; 2 μg/mL), anti-RUNX2 rabbit polyclonal antibody (ab23981, Abcam; 1:100), or anti-DMP1 rabbit polyclonal antibody (generously provided by Dr. Chunlin Qin, Texas A&M University College of Dentistry; 1:400. The immunohistochemistry experiments were detected with a 3, 3-diaminobenzidine kit (Vector Laboratories, Burlingame, CA). The immunofluorescent signals were detected with corresponding Alexa second antibody (Thermofisher, 1:200) at room temperature for 2 hours.

Histomorphometric Analyses

The region of interest (ROI) in this study was defined as the periodontal tissue in the middle third fraction of the distal area of the maxillary first molar mesial root. On the OTM side, the PDL in the ROI underwent orthodontic tensive force. Histomorphometric measurements were performed using ImageJ software (National Institutes of Health). The ratio of Axin2-lacZ^{+} area to the total ROI area were calculated (Cai et al. 2020). Next, the ALP-positive area ratio and mean integral optical density (IOD) were quantified (Hu et al. 2018). At least four slides from each sample were used for quantification.

Micro–Computed Tomography (μCT) Analysis

Maxillae were scanned by a μCT 35 imaging system (Scanco Medical, Bassersdorf, Switzerland). X-ray tube potential of 55 kV and intensity of 145 μA were applied when scanning all the samples. The voxel size was 6 μm and integration time was 800 ms. Three-dimensional reconstruction and sagittal section images were acquired by Imaris 9.0 (Bitplane).

References

Cai Y, Zhou H, Zhu Y, Sun Q, Ji Y, Xue A, Wang Y, Chen W, Yu X, Wang L et al. 2020. Elimination of senescent cells by beta-galactosidase-targeted prodrug attenuates inflammation and restores physical function in aged mice. Cell Res. 30(7):574-589.

Hu Z, Ma C, Rong X, Zou S, Liu X. 2018. Immunomodulatory ecm-like microspheres for accelerated bone regeneration in diabetes mellitus. ACS Appl Mater Interfaces. 10(3):2377-2390.

Leucht P, Kim JB, Wazen R, Currey JA, Nanci A, Brunski JB, Helms JA. 2007. Effect of mechanical stimuli on skeletal regeneration around implants. Bone. 40(4):919-930.

Men Y, Wang Y, Yi Y, Jing D, Luo W, Shen B, Stenberg W, Chai Y, Ge W-P, Feng JQ et al. 2020. Gli1+ periodontium stem cells are regulated by osteocytes and occlusal force. Developmental Cell.

Zhang H, Jiang Y, Qin C, Liu Y, Ho SP, Feng JQ. 2015. Essential role of osterix for tooth root but not crown dentin formation. J Bone Miner Res. 30(4):742-746.

Supplementary Figures

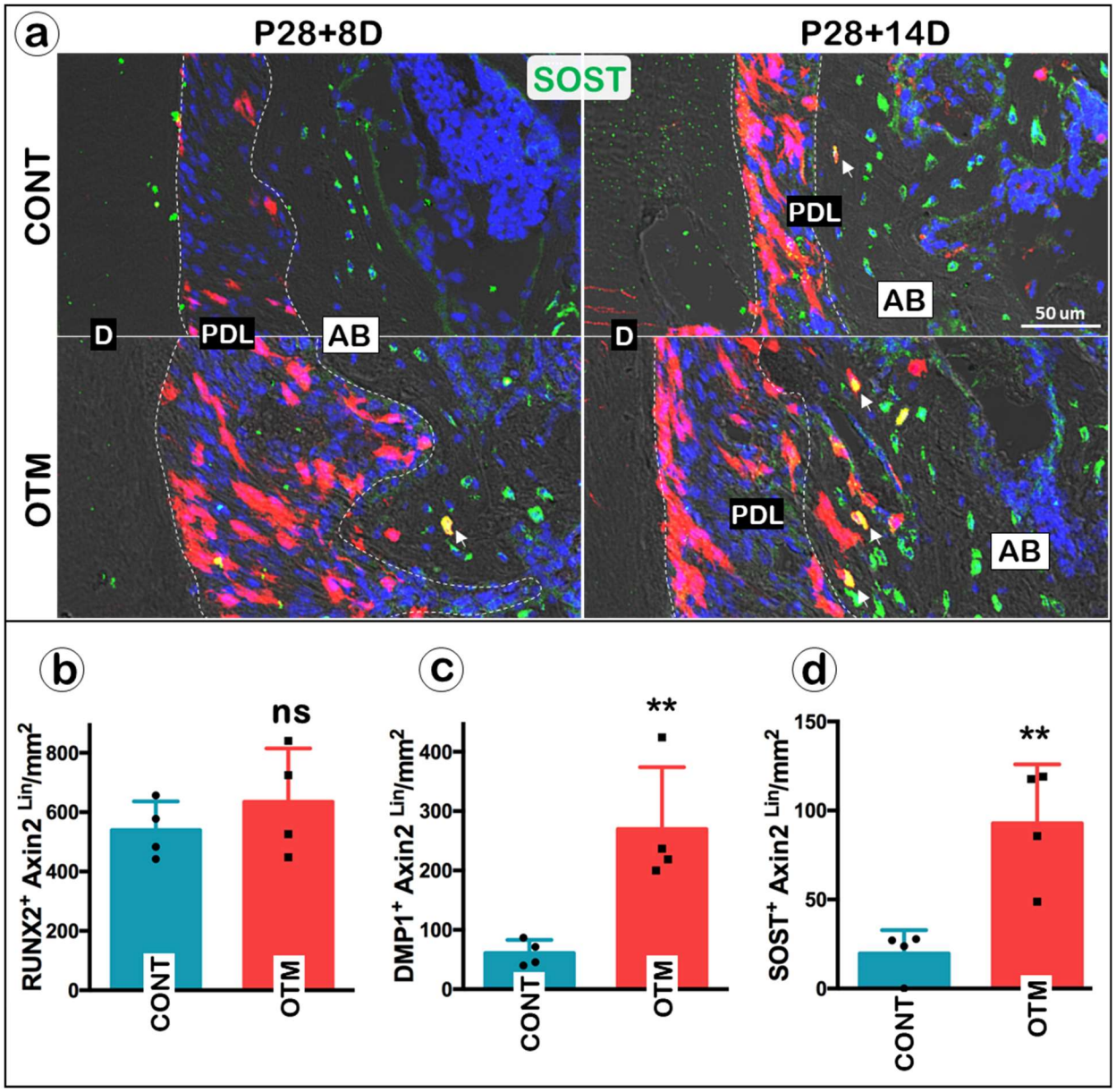

Appendix Figure.1 (**a**) Co-localization of Axin2^{+} red progeny cells with SOST immunostaining (green, white arrows). AB, alveolar bone; D, dentin; PDL, periodontal ligament. Quantification of RUNX2^{+} Axin2^{Lin}/mm^{2} in the PDL space (**b**), DMP1^{+} Axin2^{Lin}/mm^{2} (**c**) and SOST^{+} Axin2^{Lin}/mm^{2} (**d**) in the alveolar bone within 50μm of distance from the PDL at P42 (+14d). Independent t-test between CONT and OTM. n = 4; ns: not significant; **P<0.01.

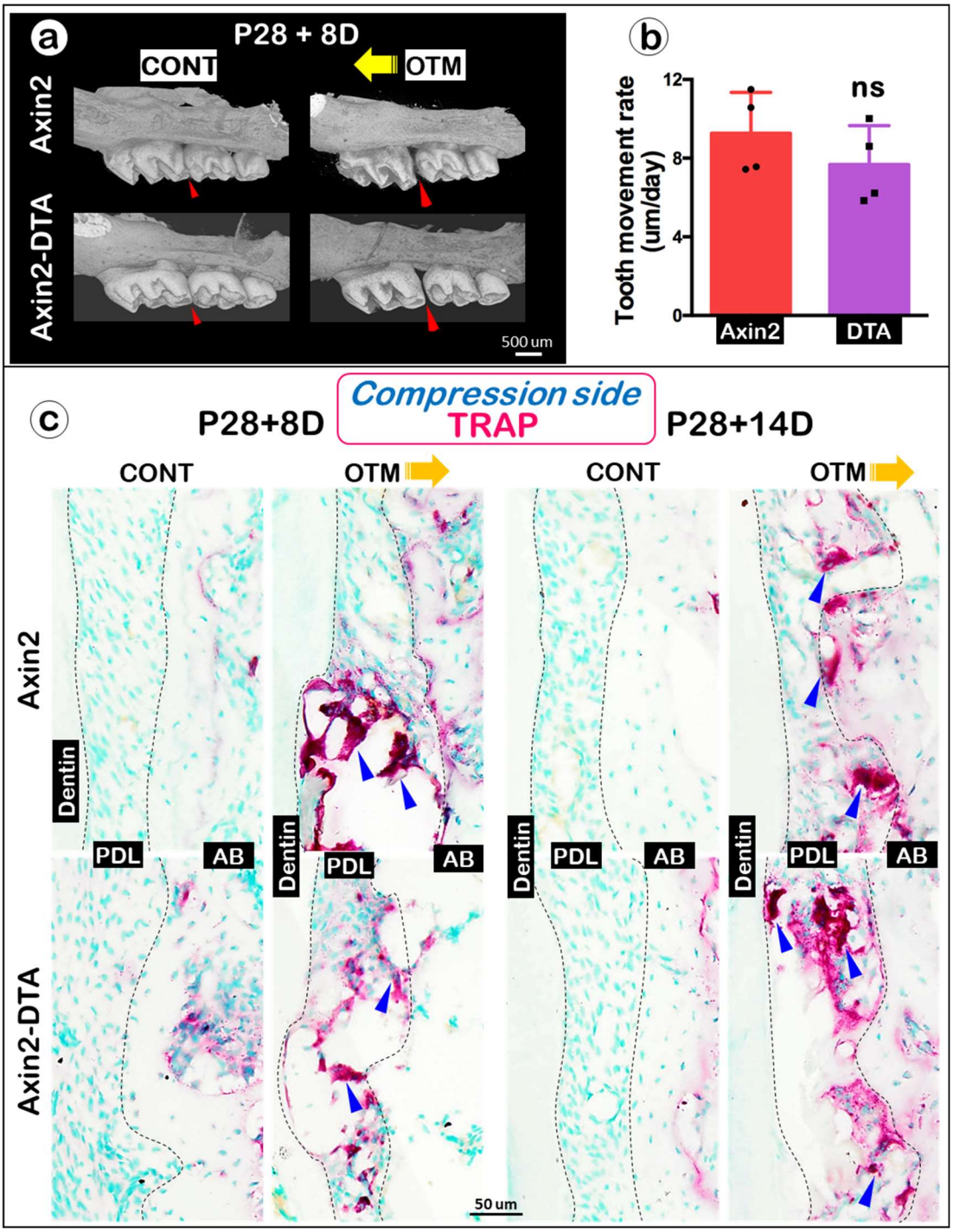

Appendix Figure.2 (**a**) Representative 3D-μCT images showed similar sizes of the gap between the first and second molars on OTM sides in the *Axin2-DTA* line (arrowhead; *lower right panel*) compared to the *Axin2* line (arrowhead; *upper right panel*) at P36 (+8d). (**b**) Quantification of tooth movement rate (μm/day). Independent t-test between *Axin2* line and *Axin2-DTA* line. n = 4; ns: not significant. (**c**) TRAP staining of the periodontium on the compression side of *Axin2* line and *Axin-DTA* line at P36 (+8d) and P42 (+14d).

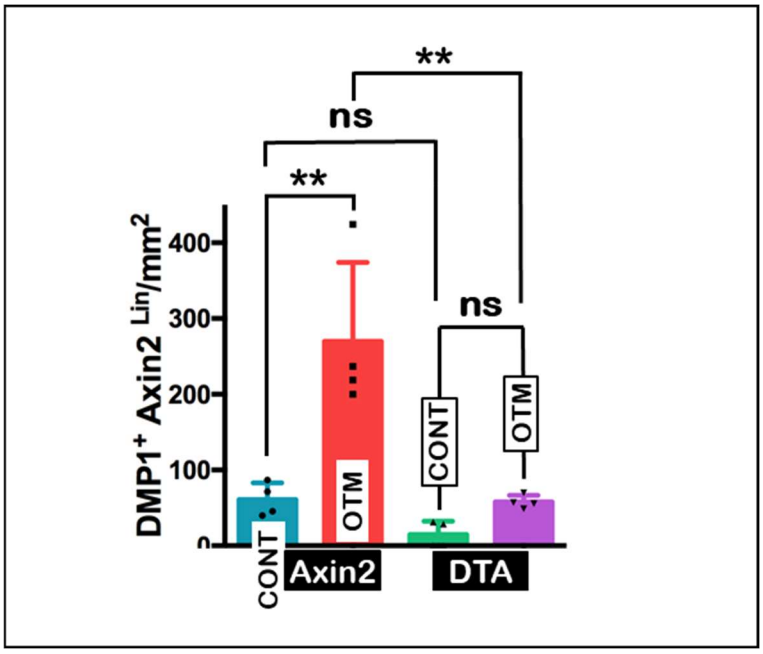

Appendix Figure.3 Quantification of DMP1^{+} Axin2^{Lin}/mm^{2} in the alveolar bone within 50μm of distance from the PDL in both the *Axin2* line and *Axin2-DTA* line at P42 (+14d). Two-way ANOVA with Tukey's post-hoc test was used. n= 4; ns: not significant; **P < 0.01.

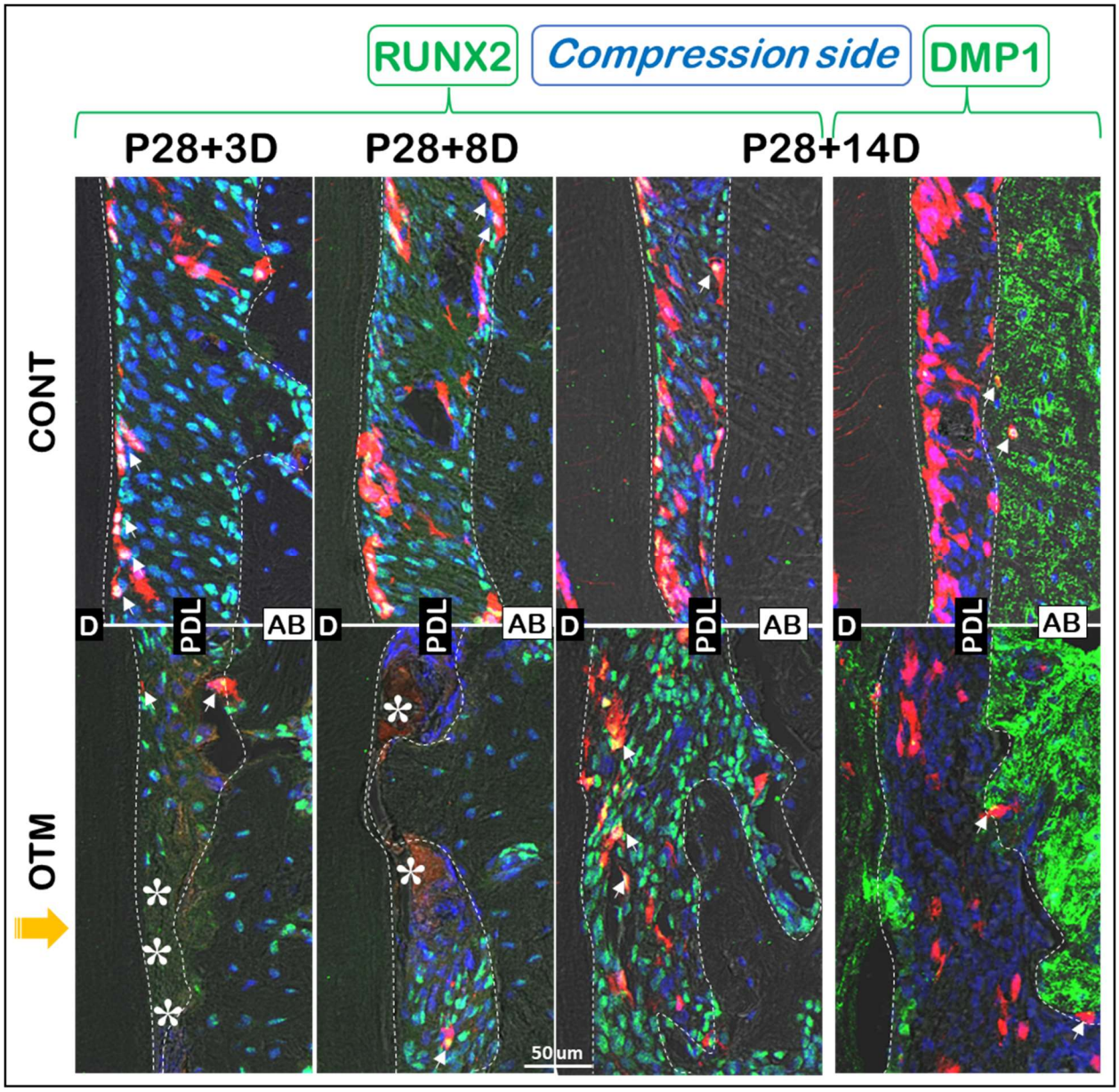

Appendix Figure.4 RUNX2 and DMP1 immunostainings of periodontal tissue on the compression side showed hyalinized zones in PDL at P31 (+3d) and P36 (+8d) (white asterisks, *lower left panels*), along with increased RUNX2^{+} Axin2^{Lin} cells and DMP1^{+} Axin2^{Lin} cells at P42 (+14d) (white arrows, *lower right panels*).